31st Annual International Conference of the IEEE EMBS
Minneapolis, Minnesota, USA, September 2-6, 2009

Effects of the electrical double layer and dispersive tissue properties in a volume conduction model of deep brain stimulation

Peadar F. Grant, *Student Member, IEEE* and Madeleine M. Lowery, *Member, IEEE*

***Abstract*—The aim of this study was to investigate the interaction of the electrode-tissue interface and dispersive tissue properties on waveforms used for deep brain stimulation. A finite element model with a distributed impedance electrical double layer was developed. Bulk tissue capacitance and dispersion were found to alter the voltage waveform under constant current stimulation. When the electrode was surrounded by conductive saline or white matter tissue, the electrical double layer was dominant under voltage controlled stimulation. However, as encapsulation tissue resistivity was increased, to emulate chronic stimulation, the voltage waveform approached that observed during constant current stimulation and the influence of the frequency dependent material properties again became dominant.**

I. Introduction

Deep brain stimulation is widely used as a clinical treatment for the symptoms of Parkinson's Disease. Despite the widespread use and success of this treatment, its mechanisms of action remain unknown. Consequently, the stimulus parameters are set largely by trial and error, which is a time-consuming process. Furthermore, stimulus parameters are assigned using non patient-specific methodologies [1].

To fully understand the mechanisms of action of DBS and to improve clinical stimulus parameter selection, it is first necessary to know the distribution of the electric potential at each point in space and time throughout the tissue immediately surrounding the electrode. The majority of bioelectric models applied to deep brain stimulation to date utilize purely resistive bulk tissue, capturing only conduction currents. Under the quasi-static approximation, capacitive, inductive and propagation effects may be neglected within the tissue at the frequencies of interest [2]. Waveforms used for deep brain stimulation are comprised of biphasic rectangular pulses, which carry energy through a wide range of frequencies. It may be necessary, therefore, to incorporate capacitive effects of the bulk neural tissue when constructing volume conduction models of DBS. This is complicated by the fact that biological materials are dispersive in nature, which means that their electrical conductivity and permittivity are themselves functions of frequency [3], [4]. For example, the relative permittivity of white matter at 100 Hz is almost 100 times that at 1 kHz [5].

Previous work has examined bulk tissue capacitive effects in deep brain stimulation [6], [7]. Frequency-dependent material properties have been investigated in other fields, including electromyography and functional electrical stimulation [8], [9]. Preliminary evidence suggests that frequency dispersion may influence models of deep brain stimulation [10]. Recent work has re-examined the validity of the quasi-static approximation when modeling electrical stimulation in homogeneous volume conductor models, suggesting that it may suffice to use quasi-static volume conductor models if the conductivity is appropriately selected [11].

When a metal electrode is placed into biological tissue, a highly resistive double layer forms at the electrode-tissue interface [12]. This interface has been approximated by a capacitor in simulation studies [13], [7]. The material properties of the encapsulation layer which forms in the peri-electrode space has been shown to affect the voltage in the tissue immediately surrounding the electrode in simulation studies [13], [14]. The effect of this layer on the interaction between the double layer and the dispersive tissue properties is not clear.

This study presents an analysis of frequency-dependent volume conduction effects of deep brain stimulation, incorporating bulk tissue with dispersive material properties, the electrode-tissue double layer, electrode encapsulation tissue and electrode geometry under constant current and constant voltage stimulation. The aim of the study was to investigate the effect of the interaction of the electrode-tissue interface and dispersive bulk tissue properties on voltage-controlled and current-controlled deep brain stimulation.

II. Methods

A frequency-domain finite element model was constructed, utilizing two geometries: an *in vitro* recording vessel and an *in vivo* idealized whole head geometry. This allowed the effect of volume conductor tissue properties and the electrode interface on the voltage waveform in the vicinity of the electrode to be examined. The *in vitro* geometry was used to verify the effect of the double-layer in isolation.

A. Geometry

The *in vitro* geometry consisted of a cylindrical saline volume conductor of diameter $7\ \mathrm{cm}$ and height $7\ \mathrm{cm}$ [15]. All outer surfaces were designated as the electrical reference, and encapsulation tissue was not present.

The whole-head geometry consisted of a set of nested ellipsoids centered around a Medtronic 3387 electrode [16]. The bulk tissue, assumed to be isotropic, occupied a volume of $0.1565\ \mathrm{m}^3$. The cerebrospinal fluid layer was $1.8\ \mathrm{mm}$ thick, calculated from its reported volume of $1.2003 \times 10^{-4}\ \mathrm{m}^3$ [17]. The skull and scalp layers were $5.5\ \mathrm{mm}$ and $4.6\ \mathrm{mm}$ thick respectively [17], [18]. The encapsulation tissue region,

This work was funded by Science Foundation Ireland Research Frontiers Programme under grant number 05/RF/ENM047.

P. F. Grant and M. M. Lowery are with the School of Electrical, Electronic and Mechanical Engineering,University College Dublin, Ireland. peadar.grant@ucd.ie

where present, was $200\ \mu\mathrm{m}$ thick. The electrical reference surface was located at the boundary at which intersects the skull, modeled as a disc of area $6.100769 \times 10^{-4}\ \mathrm{m}^2$.

B. Governing equation

The system was governed by the time-harmonic formulation of the Laplace equation, where ϕ was the dependent electric potential, considered for three formulations: resistive, capacitive and dispersive.

The resistive case considered only conduction currents:

$$-\nabla \cdot (\sigma)\nabla\phi = 0 \tag{1}$$

where σ denotes the electrical conductivity. The capacitive case considered also the displacement currents:

$$-\nabla \cdot (\sigma + j\omega\epsilon_r)\nabla\phi = 0 \tag{2}$$

where ϵ_r denotes the relative permittivity. In this study, the electrical conductivity and the relative permittivity for the resistive and capacitive models were evaluated at $1\ \mathrm{kHz}$.

To fully incorporate dielectric dispersion, at each component frequency the constants defining the electrical conductivity and relative permittivity were replaced by their Cole-Cole dispersion functions as described by Gabriel *et al* [5], Equation 3.

$$-\nabla \cdot (\sigma(\omega) + j\omega\epsilon_r(\omega))\nabla\phi = 0 \tag{3}$$

To separate out the effects of dispersion in the conductivity and relative permittivity under constant current stimulation, the electrical conductivity was allowed to vary with frequency whilst the relative permittivity was fixed at its value at 1 kHz, Equation 4. Similarly the relative permittivity was varied whilst the electrical conductivity remained fixed, Equation 5.

$$-\nabla \cdot (\sigma(\omega) + j\omega\epsilon_r(\omega_0))\nabla\phi = 0 \tag{4}$$

$$-\nabla \cdot (\sigma(\omega_0) + j\omega\epsilon_r(\omega))\nabla\phi = 0 \tag{5}$$

C. Material properties

Bulk tissue properties were assigned based on values reported in Gabriel *et al* [5]. The conductivity of saline was taken to be $1.6\ \mathrm{S/m}$ [15].

The encapsulation region was considered for three different cases: acute, not present and chronic. In the acute case, the encapsulation region consisted of purely conductive saline. When encapsulation tissue was not present the region was assigned the same material properties as the surrounding bulk tissue. The chronic case considered purely resistive encapsulation tissue of conductivity $0.0125\ \mathrm{S/m}$.

D. Boundary conditions

In constant-current models, the normal component of the current density $\hat{n} \cdot \vec{J}$ on the electrode surface was specified as:

$$\hat{n} \cdot \vec{J} = 1\ \mathrm{A/m^2} \tag{6}$$

In the constant voltage models, a distributed impedance boundary condition was used which incorporated tangential derivative variables to approximate the thin homogeneous electrical double layer [19]. The double-layer was assumed to be $100\ \mathrm{nm}$ thick and was implemented using a thin layer approximation [12]. An electric potential of $1\ \mathrm{V}$ was applied to the electrode. The electric potential on the electrical reference surfaces was set to zero volts. The normal component of the current density was conserved at interior boundaries.

E. Solution

The model was constructed, discretized and solved using COMSOL Multiphysics 3.5a (COMSOL Ltd., Hertfordshire, United Kingdom).

The idealized geometry was discretized into 332,849 tetrahedral elements using Delaunay triangulation. Linear element shape functions were extended onto each element, resulting in 60,223 degrees of freedom in the system matrix. The minimum element edge length was $8.8 \times 10^{-5}\ \mathrm{m}$. Mesh density and element quality of the *in vitro* mesh were similar to those in the idealized anatomical mesh.

The PARDISO linear solver calculated the amplitude and phase response at each point within both geometries at 2000 component frequencies from $0\ \mathrm{Hz}$ to $259,870\ \mathrm{Hz}$ at intervals of $130\ \mathrm{Hz}$.

F. Postprocessing

The transfer function $H(j\omega)$ from DC to $260\ \mathrm{kHz}$ was calculated from the finite element model at a point $3\ \mathrm{mm}$ from the electrode. The representative distance of $3\ \mathrm{mm}$ was chosen as it is within the volume of the subthalamic nucleus. The stimulus $x(t)$ was synthesized in the time domain from its trigonometric Fourier series. The pulse width, except where otherwise stated, was $100\ \mu\mathrm{s}$. It was converted into its one-sided frequency spectrum, $X(j\omega)$, using the Fast Fourier Transform (FFT). This was then multiplied by $H(j\omega)$ to yield the frequency spectrum $Y(j\omega)$. The inverse FFT of $Y(j\omega)$ yields the temporal voltage waveform $y(t)$ at the point of interest, $3\ \mathrm{mm}$ from the electrode.

III. Results

The simulated *in vivo* waveforms predicted by the resistive, capacitive and dispersive models under constant current stimulation are presented in Fig. 1.

Changing the frequency at which the conductivity and permittivity were estimated elicited root mean square (RMS) errors of up to 58% with respect to the *in vivo* fully dispersive model in the case of the *in vivo* capacitive model with material properties calculated at $100\ \mathrm{Hz}$ under constant current stimulation, Fig. 2.

The simulated *in vivo* voltage waveforms predicted by the fixed permittivity-dispersive conductivity (Disp. σ) fixed conductivity-dispersive permittivity (Disp. ϵ), and full dispersive models, are shown in Fig. 3.

The RMS error of the simulated *in vitro* voltage waveforms resulting from the Disp. σ and Disp. ϵ tissue models with respect to the that resulting from the fully dispersive model were up to 28% and 8%, respectively, for pulse widths in the range $50\ \mu\mathrm{s}$ to $550\ \mu\mathrm{s}$, Fig. 4.

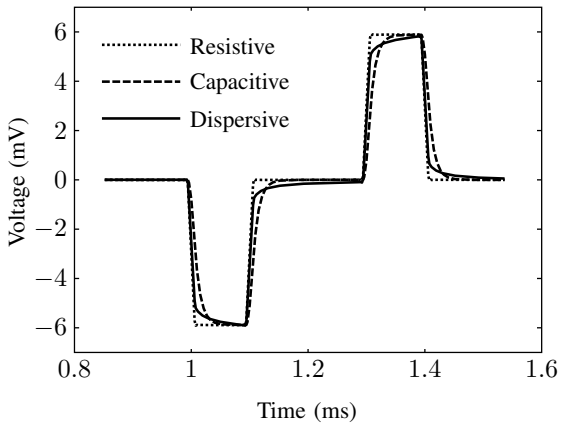

Fig. 1. Simulated *in vivo* electric potential under constant current stimulation at 3mm from the stimulating electrode contact for resistive, capacitive and dispersive bulk tissue properties. The electrode was directly coupled to the bulk tissue. Encapsulation tissue was not present.

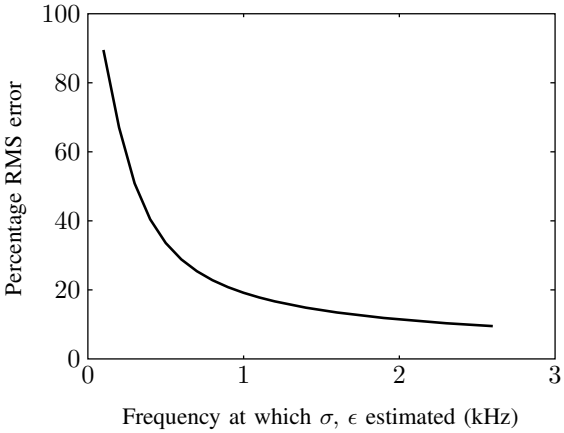

Fig. 2. Percentage root mean square error of *in vivo* voltage waveform resulting from capacitive bulk tissue properties to that resulting from dispersive tissue properties.

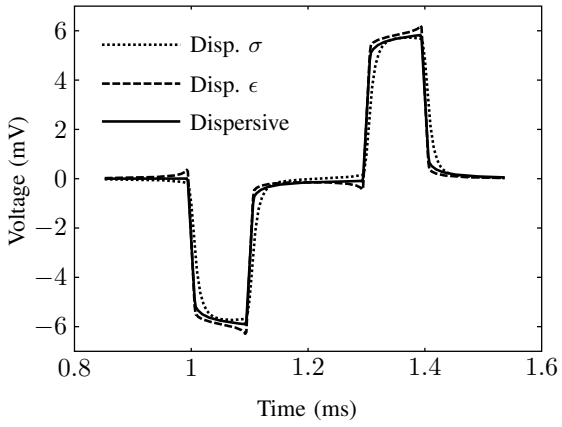

Fig. 3. Simulated *in vivo* voltage waveforms under constant current stimulation 3 mm from the stimulating electrode contact for fixed permittivity-dispersive conductivity, fixed conductivity-dispersive permittivity and fully dispersive bulk tissue properties. The electrode was directly coupled to the bulk tissue. Encapsulation tissue was not present.

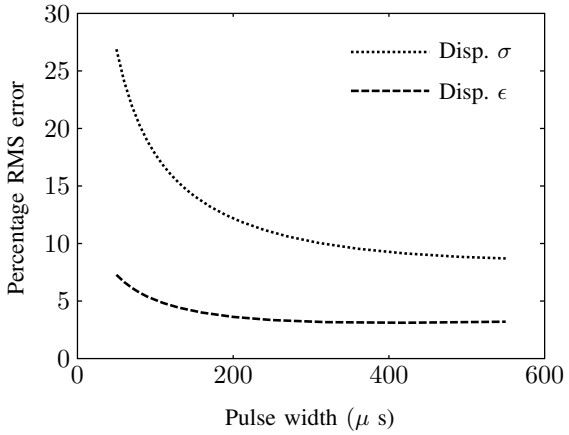

Fig. 4. Percentage root mean square error of fixed permittivity-dispersive conductivity and fixed conductivity-dispersive permittivity bulk tissue properties with respect to fully dispersive bulk tissue properties over pulse widths ranging from 50 μs to 550 μs.

To quantify the effect of the electrical double layer in isolation, the *in vitro* electric potential was examined at a point 3 mm from the electrode under constant current stimulation, Fig. 5.

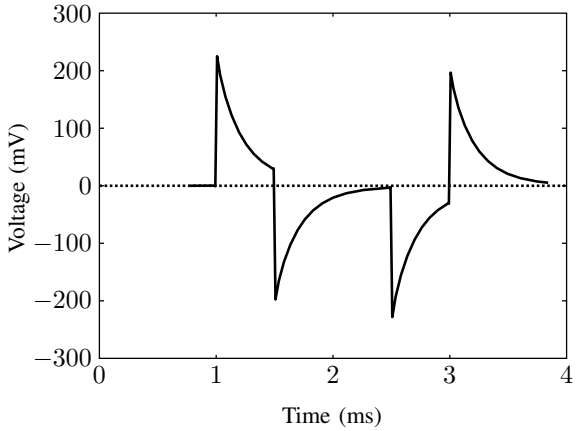

Fig. 5. Simulated *in vitro* electric potential under constant voltage stimulation (pulse width 500 μs) at 3 mm from the stimulating electrode contact for resistive saline bulk tissue medium. The electrode and tissue are coupled by an electrical double-layer. Encapsulation tissue was not present.

The simulated *in vivo* voltage waveforms due to constant voltage stimulation were normalized and are shown in Fig. 6.

IV. Discussion

The tissue frequency response differed in both magnitude and shape among the resistive, capacitive and dispersive models, causing variations in the simulated *in vivo* voltage waveforms at a representative point in the tissue surrounding the electrode located 3 mm from the stimulating contact.

The RMS error between the *in vivo* voltage waveform calculated using non-dispersive capacitive bulk tissue properties and that calculated using fully dispersive properties decreased as the frequency at which material properties were

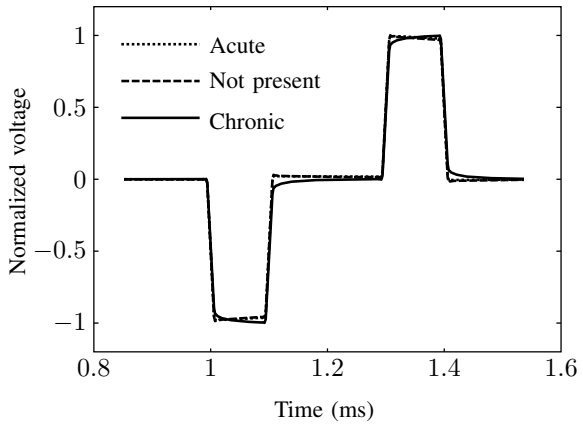

Fig. 6. Simulated *in vivo* normalized voltage waveform under constant voltage stimulation at $3\,\mathrm{mm}$ from the stimulating electrode contact for dispersive bulk tissue properties. The electrode is coupled to the bulk tissue medium by an electrical double layer. Encapsulation tissue is modeled as acute ($\sigma = 1.6\ \mathrm{S/m}$), not present and chronic ($\sigma = 0.0125\ \mathrm{S/m}$).

calculated was increased. It became horizontally asymptotic at an error of approximately 9%. Non-dispersive capacitive solutions showed greater RMS errors than resistive solutions with respect to fully dispersive material properties. Additionally, use of the dispersive bulk tissue properties removes the need to make an arbitrary or unsystematic parameter selection in order to estimate capacitive effects.

Furthermore, the RMS error of *in vivo* voltage waveforms resulting from dispersion in one single parameter (Disp. σ and Disp. ϵ) with respect to that from the fully dispersive model suggest that it is of particular importance that the frequency dependence of the relative permittivity is explicitly incorporated, Fig. 4.

Under constant current stimulation, the simulated *in vitro* voltage waveform was shown to be affected by the electrical double layer, Fig. 5. The double-layer incorporated in the model was found to agree with experimentally measured voltage waveforms.

Simulations conducted *in vivo* which considered constant voltage stimuli coupled to the bulk tissue by an electrical double-layer showed that the interaction between the double-layer and the dispersive bulk tissue properties was dependent on the nature of the encapsulation layer surrounding the electrode, Fig. 6. The influence of the electrical double layer was dominant when the electrode was surrounded by purely conductive saline, or where the encapsulation layer was nonexistent. The influence of the dispersive tissue properties was dominant when the electrode was surrounded by chronic purely resistive encapsulation tissue.

V. Conclusion

A model was developed, to examine the frequency-dependent effects and interactions of the electrical double layer interface and dispersive material properties in the surrounding tissue. It was found that incorporating dispersion in bulk tissue material properties affected the shape of the waveforms predicted by capacitive solutions under constant current stimulation Under constant voltage stimulation, the effect of dispersion in the bulk tissue was dependent on the properties of the electrode encapsulation layer. When encapsulation tissue was not present and when the peri-electrode space was filled with saline, the effect of the electrical double layer was dominant. However, when the electrode was surrounded by highly resistive encapsulation tissue the effect of the bulk tissue again became dominant.

References

[1] J. Volkmann, J. Herzog, F. Kopper, and G. Deuschl, "Introduction to the programming of deep brain stimulators." *Mov Disord*, vol. 17 Suppl 3, pp. S181–7, 2002.

[2] R. Plonsey and D. B. Heppner, "Considerations of quasi-stationarity in electrophysiological systems." *Bull Math Biophys*, vol. 29, no. 4, pp. 657–664, 1967.

[3] C. Gabriel, S. Gabriel, and E. Corthout, "The dielectric properties of biological tissues: I. literature survey." *Phys Med Biol*, vol. 41, no. 11, pp. 2231–2249, 1996.

[4] S. Gabriel, R. W. Lau, and C. Gabriel, "The dielectric properties of biological tissues: Ii. measurements in the frequency range 10 hz to 20 ghz." *Phys Med Biol*, vol. 41, no. 11, pp. 2251–2269, 1996.

[5] ——, "The dielectric properties of biological tissues: Iii. parametric models for the dielectric spectrum of tissues." *Phys Med Biol*, vol. 41, no. 11, pp. 2271–2293, 1996.

[6] C. R. Butson and C. C. McIntyre, "Tissue and electrode capacitance reduce neural activation volumes during deep brain stimulation." *Clin Neurophysiol*, vol. 116, no. 10, pp. 2490–2500, 2005.

[7] N. Yousif, R. Bayford, and X. Liu, "The influence of reactivity of the electrode-brain interface on the crossing electric current in therapeutic deep brain stimulation." *Neuroscience*, vol. 156, no. 3, pp. 597–606, 2008 Oct 15.

[8] N. S. Stoykov, M. M. Lowery, A. Taflove, and T. A. Kuiken, "Frequency- and time-domain fem models of EMG: capacitive effects and aspects of dispersion." *IEEE Trans Biomed Eng*, vol. 49, no. 8, pp. 763–772, 2002.

[9] L. Mesin and R. Merletti, "Distribution of electrical stimulation current in a planar multilayer anisotropic tissue." *IEEE Trans Biomed Eng*, vol. 55, no. 2 Pt 1, pp. 660–670, Feb 2008.

[10] P. F. Grant and M. M. Lowery, "Tissue dispersion in an inhomogeneous model of dbs," in *Neuroscience 2008, Washington DC, USA*, 2008.

[11] C. A. Bossetti, M. J. Birdno, and W. M. Grill, "Analysis of the quasi-static approximation for calculating potentials generated by neural stimulation." *J Neural Eng*, vol. 5, no. 1, pp. 44–53, 2008 Mar.

[12] D. R. Cantrell, S. Inayat, A. Taflove, R. S. Ruoff, and J. B. Troy, "Incorporation of the electrode-electrolyte interface into finite-element models of metal microelectrodes." *J Neural Eng*, vol. 5, no. 1, pp. 54–67, 2008.

[13] C. R. Butson, C. B. Maks, and C. C. McIntyre, "Sources and effects of electrode impedance during deep brain stimulation." *Clin Neurophysiol*, vol. 117, no. 2, pp. 447–454, 2006.

[14] N. Yousif, R. Bayford, P. G. Bain, and X. Liu, "The peri-electrode space is a significant element of the electrode-brain interface in deep brain stimulation: a computational study." *Brain Res Bull*, vol. 74, no. 5, pp. 361–368, 2007.

[15] S. Miocinovic, S. Lempka, G. Russo, C. Maks, C. Butson, K. Sakaie, J. Vitek, and C. McIntyre, "Experimental and theoretical characterization of the voltage distribution generated by deep brain stimulation." *Exp Neurol*, 2008 Dec 11.

[16] Medtronic, Inc., *3387-3389 Lead Kit for Deep Brain Stimulation - Implant Manual*, Minneapolis, MA, 2006.

[17] International commission of radiological protection, *Report of the Task Group on Reference Man*. Oxford Pergamon Press, 1975.

[18] O. Scheufler, N. M. Kania, C. M. Heinrichs, and K. Exner, "Hyperplasia of the subcutaneous adipose tissue is the primary histopathologic abnormality in lipedematous scalp." *Am J Dermatopathol*, vol. 25, no. 3, pp. 248–252, 2003.

[19] X. Huang, D. Nguyen, D. Greve, and M. Domach, "Simulation of microelectrode impedance changes due to cell growth," *Ieee Sensors Journal*, vol. 4, no. 5, pp. 576–583, OCT 2004.